Mechanically induced gelation of a kinetically trapped supramolecular polymer

Macromolecules

Article

pubs.acs.org/Macromolecules

Mechanically Induced Gelation of a Kinetically Trapped Supramolecular Polymer

Abraham J. P. Teunissen, Marko M. L. Nieuwenhuizen, Fransico Rodríguez-Llansola, Anja R. A. Palmans, and E. W. Meijer*

Laboratory of Macromolecular and Organic Chemistry, Eindhoven University of Technology, P.O. Box 513, NL-5600 MB Eindhoven, The Netherlands

Supporting Information

ABSTRACT: The stimuli-induced gelation of a urethane-functionalized ditopic ureidopyrimidinone (UPy) compound is presented, and the mechanism by which the gelation proceeds is proposed. In a 40−120 mM solution in chloroform, the compound can exist in two different aggregated states, namely a low viscous mixture of (cyclic) oligomers or a fibrous gel. As evidenced by IR, NMR, and WAXS, the liquid state is stabilized by hydrogen bonds between the UPy and the back-folded chain, while the fibrous gel is stabilized by lateral hydrogen bonds within stacked UPy dimers. Controlled preparation techniques allow for pathway selection to arrive at one of both states. The remarkable long-term stability of the low viscous state (over 2 months for a 80 mM solution) is in contrast to the fast transformation into a gel by stirring in a few hours. Other mechanical stimuli like shaking, sonicating, and stirring for a shorter period, as well as freezing and thawing the solution, yield weaker gels than those obtained by long stirring. Heating the gels and slow cooling reversibly yield the nonviscous solution. This shows that the formation of UPy−urethane hydrogen bonds kinetically traps the UPy polymers, thereby preventing their lateral aggregation. The application of mechanical stress or freezing disrupts this interaction, allowing for the formation of a stacked nucleus on which further material can grow, eventually leading to gelation of the solution.

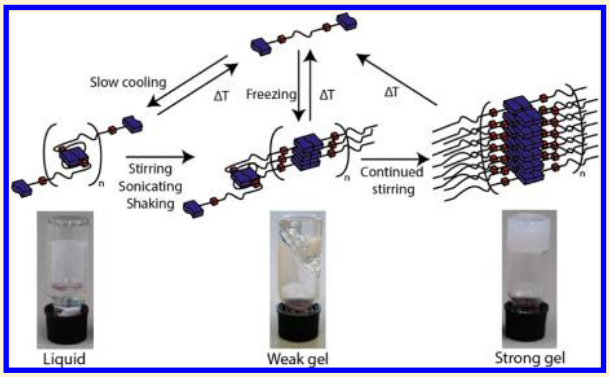

INTRODUCTION

External stimuli such as temperature, pH, or light are widely used to influence material properties.[1−3] Particularly interesting are mechanical forces; the aligning of polymeric chains by stretching,[4] inducing symmetry breaking by stirring a solution during crystallization,[5,6] influencing the charge transport properties of semiconductors by shear stress during fabrication,[7] and the shear-induced gelation of a mixture of telechelic polymers[8] are examples that highlight their potential. The behavior of supramolecular systems is sensitive to external stimuli as well, and many elegant examples using a variety of external stimuli have been presented.[9−11]

An intriguing research area is the switching of nonaggregated precursors into aggregated structures to induce gel formation. Examples of gelation induced by stirring or shaking often make use of colloidal suspensions.[12,13] Moreover, the shear-induced formation of a copper metallogel[14] and the gelation of a small organic compound under the influence of shaking[15] have been observed in synthetic molecular systems. Especially interesting is a reported system where different thermo-, chemo-, and mechanical stimuli lead to gels of different strength.[16] Frequently, gelation is initiated by disruption of an intramolecular interaction, allowing the formation of a nucleus on which further material can grow.[17] In many cases, however, the exact underlying mechanisms are not well understood. Recently, our group reported on the autoregulatory behavior of a urethane-functionalized ditopic ureidopyrimidinone (urethane-UPy) compound **1** (Figure 1) on the catalytic activity of 2,7-diamido-1,8-naphthyridine in a Michael addition.[18] During the course of these investigations, we discovered that solutions of compound **1** in $CHCl_3$ became thixotropic under the influence of mechanical agitation or freezing. Preliminary molecular modeling studies (Figure 1) suggested that this observation can be related to the presence of an intramolecular UPy−urethane hydrogen bond in monomeric **1**.

We herein report our detailed studies on the stimuli-induced gelation of urethane-UPy **1**, with the aim to understand the mechanism by which the gelation proceeds. As a reference, we study ester-UPy **2**, which lacks the urethanes and, as a result, also the ability to form a similar intramolecular hydrogen bond. Remarkably, the application of different types of stimuli on solutions of **1** (temperature or mechanical forces) results in different outcomes: either a nonviscous solution or gels of different strengths (Figure 2). The different states of **1** were studied with a combination of NMR, IR, rheology, and WAXS,

Received: October 3, 2014
Revised: November 10, 2014
Published: December 1, 2014

   dx.doi.org/10.1021/ma502047h | Macromolecules 2014, 47, 8429−8436

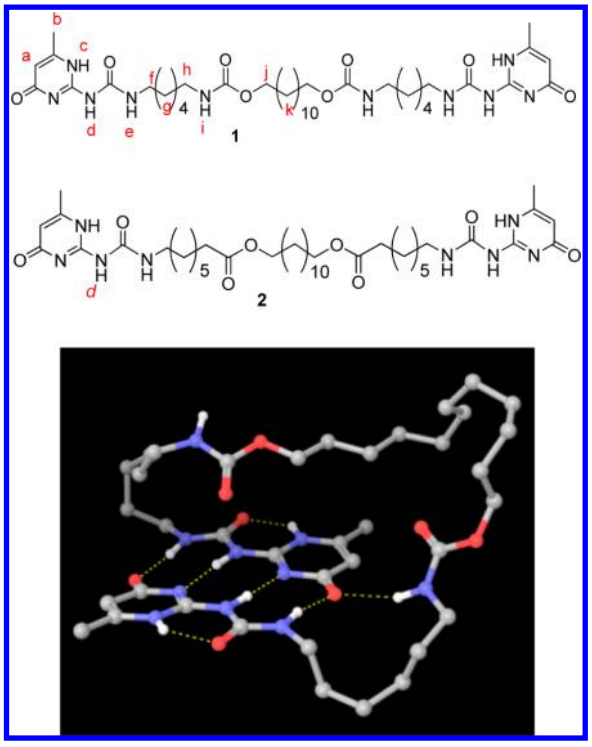

Figure 1. Upper frame: molecular structure of **1** and **2**. Lower frame: minimized conformation of a monomeric cycle of **1**.

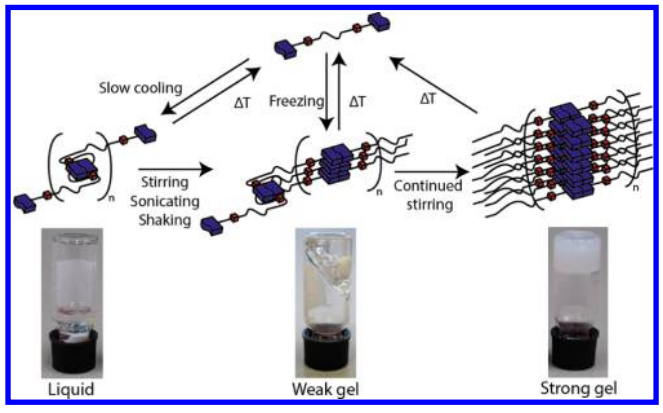

Figure 2. Influence of external stimuli on the self-assembly of **1** in $CHCl_3$. Slowly cooling the hot solution results in a nonviscous liquid. Shaking or sonicating for any period of time or stirring for up to 30 min results in a transparent, weak gel. A similar weak gel is obtained by quickly freezing the solution in liquid N_2. Weak gels formed by any of these procedures can be converted into nontransparent stronger gels by stirring for an extended period of time (±3 h). UPy groups are represented by blue squares while red squares represent the urethane groups. Cyclic structures have been omitted from the cartoon.

the results of which reveal that a UPy–urethane hydrogen bond is present in solution but is absent in the gel. On the basis of these results, we propose a mechanism that rationalizes the mechanically and temperature-induced gelation.

EXPERIMENTAL SECTION

Materials and Methods. All used solvents were of analytical grade; all chemicals were purchased from Sigma-Aldrich and used without further purification. Immobilized *Candida Antarctica* Lipase B (Novozym 435) was obtained from Novozymes A/S. Unless noted otherwise, all measurements were performed in chloroform. Unless noted otherwise, all gels were made by the following procedure: The compound was suspended in 1 mL of chloroform in a 32 × 11.6 mm vial; this was heated until the compound was completely dissolved and then allowed to cool to room temperature. The obtained solution was then stirred for 3 h at 900 rpm using a 6 × 1 mm stirring bar, followed by a resting time of at least 2 h. Deconvolution of NMR spectra was performed using MestReNova software version 7.1.1-9649. All liquid NOE/ROE samples were degassed by the application of three freeze–pump–thaw cycles. Data processing was performed using VNMRJ.3.2.a software. All nonpulse field gradient ^1H and ^{13}C NMR spectra were recorded on a Varian Mercury 400 MHz NMR, while all pulse field gradient measurements (i.e., NOE/ROE/DOSY) were recorded on a 500 MHz Varian Unit Inova. All NMR measurements were conducted at 25 °C. Polarized optical microscopy (POM) was performed on a Sondag Optische Instrumenten microscope. Simulations were performed using Maestro software version 9.4, the structures were minimized using an AMBER force field in chloroform, hydrogen bonding atoms were connected using flexible constrains.

Synthetic Procedures and Characterization. 8-((*tert*-Butoxycarbonyl)amino)octanoic Acid (4). 8-Aminooctanoic acid (3.0 g, 18.8 mmol) was dissolved in a mixture of DCM (5 mL) and water (5 mL). NaOH (1.5 g, 37.5 mmol) was added, and the solution was cooled to 0 °C. A solution of di-*tert*-butyldicarbonate (4.1 g, 18.8 mmol) in DCM (20 mL) was slowly added, and the reaction mixture was stirred for 24 h at room temperature. The solution was acidified using concentrated HCl (3 mL), and the aqueous phase was extracted with DCM (2 × 40 mL). The combined organic phases were dried using $MgSO_4$, and the solvent was removed under vacuum. Yield: 2.32 g, 8.97 mmol. η: 47.6%. ^1H NMR (400 MHz; $CDCl_3$) δ: 9.2 (1H, bs, COOH), 4.54 (1H, s, NH), 3.09 (2H, m, NH–CH_2), 2.33 (t, CO–CH_2), 1.66 (NH–CH_2–CH_2), 1.44 (11H, m, CH_3, CH_2), 1.32 (6H, m, CH_2). ^{13}C NMR (100 MHz, $CDCl_3$) δ: 179.12, 155.99, 79.10, 40.53, 33.95, 29.93, 28.92, 28.40, 26.53, 24.58. MALDI-TOF-MS: calcd mass 259.18 g/mol; found 282.27 g/mol $(M + Na)^+$.

Dodecane-1,12-Diyl Bis(8-((*tert*-butoxycarbonyl)amino)-octanoate) (5). 8-((*tert*-Butoxycarbonyl)amino)octanoic acid (142 mg, 0.548 mmol) and dodecane-1,12-diol (55 mg, 0.272 mmol) were dissolved in hexane (5 mL), and Novozym 435 beads (15 mg) were added. The solution was put on a rotary evaporator and gently rotated for 3 h at 70 °C at a pressure of 800 mbar. When necessary, extra hexane was added. The solution was cooled down, hexane (20 mL) was added, and the enzyme beads were filtered off and rinsed with additional hexane. The solvent was evaporated under vacuum to yield the desired compound. Yield: 185 mg, 0.27 mmol. η: 99%. ^1H NMR (400 MHz; $CDCl_3$) δ: 4.48 (2H, bs, NH), 4.05 (4H, t, O–CH_2), 3.11 (4H, m, N–CH_2), 1.62 (8H, m, CH_2), 1.44 (22H, m, CH_3, CH_2), 1.31 (28H, m, CH_2). ^{13}C NMR (100 MHz, $CDCl_3$) δ: 173.89, 155.97, 79.02, 64.41, 40.52, 34.31, 30.00, 29.53, 29.50, 29.24, 29.03, 28.91, 28.64, 28.42, 26.60, 25.91, 24.88. MALDI-TOF-MS: calcd mass 684.53 g/mol; found 707.53 g/mol $(M + Na)^+$.

8,8′-(Dodecane-1,12-diylbis(oxy))bis(8-oxooctan-1-aminium) 2,2,2-Trifluoroacetate (6). Dodecane-1,12-diyl bis(8-((*tert*-butoxycarbonyl)amino)octanoate) (193 mg, 0.28 mmol) was dissolved in a solution of 30% TFA in DCM (10 mL total). The mixture was stirred at room temperature for 3 h. The solvents were coevaporated with toluene (2 × 5 mL) to yield the desired product. Yield: 137 mg. η: 99.6%. ^1H NMR (400 MHz; $CDCl_3$) δ: 7.86 (6H, bs, NH_3^+), 4.09 (4H, t, O–CH_2), 2.98 (4H, bs, N–CH_2), 2.32 (4H, t, C═O–CH_2), 1.75–1.54 (12H, m, CH_2), 1.47–1.21 (28H, m, CH_2). ^{13}C NMR (100 MHz, $CDCl_3$) δ: 174.38, 67.06, 39.95, 34.23, 29.51, 29.05, 28.83, 28.42, 28.32, 27.25, 25.72, 24.56. MALDI-TOF-MS: calcd mass 684.99 g/mol; found 486.46 g/mol (monoprotonated diamine without TFA).

***N*-(6-Methyl-4-oxo-1,4-dihydropyrimidin-2-yl)-1*H*-imidazole-1-carboxamide (7).** 2-Amino-6-methylpyrimidin-4(1*H*)-one (1.0 g, 7.99 mmol) was dissolved in DMSO (10 mL), di(1*H*-imidazol-1-yl)methanone (1.68 g, 10.36 mmol) was added, and the mixture was stirred for 24 h at 80 °C. The solution was cooled to room temperature, and acetone was added to precipitate the product. The precipitate was filtered, and the residue washed with acetone. The product was dried under vacuum to yield the desired product. Yield: 1.59 g, 7.25 mmol. η: 91%. Note: due to its extremely low solubility in

dx.doi.org/10.1021/ma502047h | *Macromolecules* 2014, 47, 8429–8436

Scheme S1. Synthetic Route toward Compound 2[a]

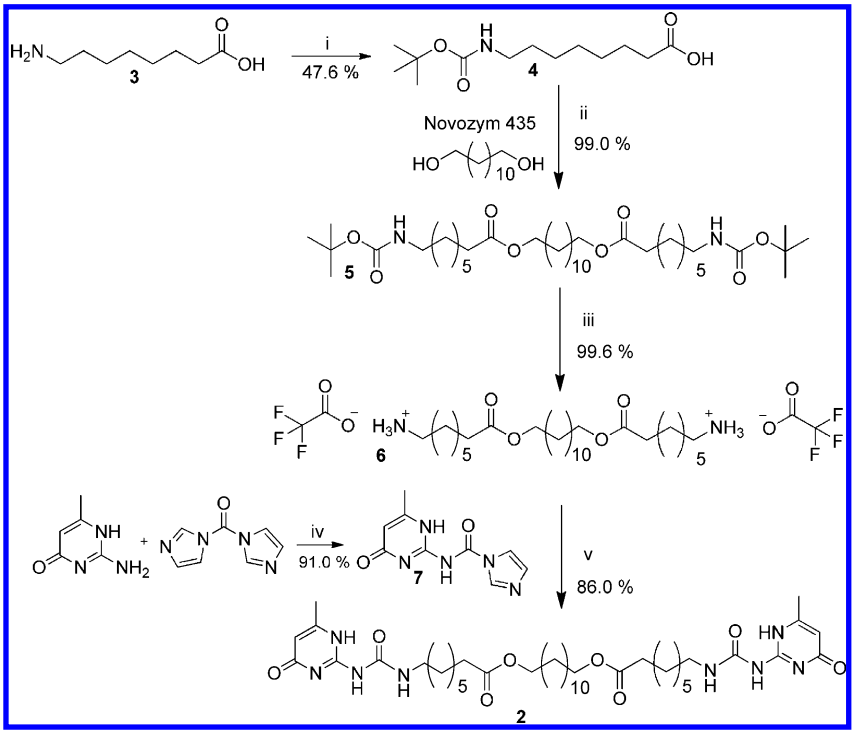

[a]Reagents and conditions: (i) DCM, H_2O, NaOH, di-*tert*-butyl dicarbonate, RT; (ii) hexane, Novozyme 435, 70 °C, 800 mbar; (iii) DCM, TFA, RT; (iv) DMSO, 80 °C; (v) DMF, triethylamine, RT.

most solvents, this compound is hard to characterize. IR (ATR): $\tilde{\nu}$ = 3175, 3075, 2648 (bs) 1701, 1645, 1601, 1509, 1479, 1375, 1334, 1320, 1276, 1233, 1224, 1190, 1169, 1090, 1065, 1026, 983 cm^{-1}.

Dodecane-1,12-diyl Bis(8-(3-(6-methyl-4-oxo-1,4-dihydropyrimidin-2-yl)ureido)octanoate) (2). 8,8′-(Dodecane-1,12-diylbis(oxy))bis(8-oxooctan-1-aminium) 2,2,2-trifluoroacetate (137 mg, 0.28 mmol) was dissolved in DMF (10 mL). Triethylamine (0.2 mL) and *N*-(6-methyl-4-oxo-1,4-dihydropyrimidin-2-yl)-1*H*-imidazole-1-carboxamide (300 mg, 1.37 mmol) were added, and the mixture was stirred at room temperature for 24 h. The solvent was removed *in vacuo*, and chloroform (50 mL) was added. The organic phase was filtered and subsequently dried under vacuum to yield the desired compound. Yield: 191 mg, 0.243 mmol. η: 86%. ^{1}H NMR (400 MHz; $CDCl_3$) δ: 13.11 (2H, s, CH_3CN-H), 11.88 (2H, s, $CH_2NH(C{=}O)NH$), 10.11 (2H, S, $CH_2NH(C{=}O)NH$), 5.81 (2H, s, $CH{=}CCH_3$), 4.05 (4H, t, $(C{=}O)O-CH_2$), 3.25 (4H, m, $NH-CH_2$), 2.22 (6H, m, CH_3), 1.54 (6H, m, CH_3), 1.55−1.20 (40H, m, CH_2). ^{13}C NMR (100 MHz, $CDCl_3$) δ: 173.92, 172.99, 156.57, 154.70, 148.16, 106.70, 64.31, 39.97, 34.34, 29.53, 29.23, 28.64, 26.41, 25.97, 24.83, 18.93. MALDI-TOF-MS: calcd mass 786.50 g/mol; found 787.52 g/mol $(M + H)^+$.

RESULTS AND DISCUSSION

Gelation Studies. Dissolution of either **1** or **2** in hot $CHCl_3$ resulted in nonviscous solutions after slow cooling. While solutions of **2** never showed an increase in viscosity in the concentrations we examined (c = 1−150 mM), solutions of **1** could be converted into gels of different strength depending on the type of stimulus applied. Figure 2 summarizes different preparation methods (slow cooling by standing under ambient conditions, quickly freezing a hot solution in liquid N_2, and the application of different mechanical forces) and how these affect the material properties of **1** in chloroform.

The different methods of mechanically agitating solutions of **1** (40−120 mM in chloroform) yielded gels that differ in appearance and mechanical properties. A transparent, weak gel is obtained after roughly 10 h as a result of shaking or sonication for several seconds as well as stirring for a short period of time (<30 min). In contrast, a much more rigid, nontransparent strong gel is formed directly by stirring for an extended period of time (±3 h). Both the weak and the strong gel showed no visible change for extended periods of time (>1 month for 80 mM gels). Upon heating the samples above 50 °C, followed by slow cooling, stable low viscous solutions (>2 months for an 80 mM solution) were obtained again. These solutions can be reconverted into weak or strong gels upon agitation, showing that the processes are fully reversible.

Surprisingly, not only mechanical agitation caused gelation of the solutions. Freezing the hot solution by immersion in liquid N_2 resulted in formation of a transparent weak gel immediately after thawing of the solvent. The gels formed via this approach were similar in appearance as those formed by shaking and sonication. Although the viscosity and rate of formation were visibly lower, weak gels could also be formed by seeding a solution of **1** (40 mM) with gel of (equal) concentration, which shows that the formation of the gels is driven by a nucleated growth mechanism. Although continued stirring is the only preparation method that results in the formation of opaque strong gels, it should be noted that also the formation of the weak transparent gels is a gradual process, and the kind and duration of the applied stimuli influence their eventual strength.

Samples containing urethane-UPy **1** at concentrations of c = 40 and 80 mM in other solvents such as tetrahydrofuran, dichloromethane, dichloroethane, toluene, or 1,2-dichlorobenzene did not gelate under the influence of stirring, likely as a result of the poor solubility of **1** in these solvents.

Liquid State Obtained after Slow Cooling. To elucidate the different conformations formed by **1** in chloroform, ^{1}H

dx.doi.org/10.1021/ma502047h | *Macromolecules* 2014, 47, 8429−8436

NMR spectra were measured at various concentrations. As shown in Figure 3, at least eight different urethane signals can be observed at c = 10 mM. The signals numbered 1, 2, 3, 6, 7, and 8 are already present at concentrations as low as 1.25 mM.

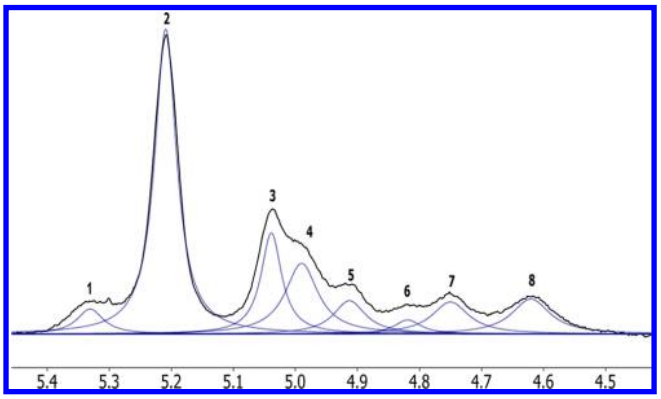

Figure 3. ^{1}H NMR spectrum of **1** at c = 10 mM, showing eight different urethane signals. The NMR spectrum is shown in black, while the deconvolution of the different signals is shown in blue.

Deconvolution of the signals allowed for the quantification of the peak areas, from which the corresponding concentrations were calculated. The concentrations corresponding to all signals except signal 5 saturate upon increasing the total concentration (Figure 4). In contrast, signal 5 displays a short period of exponential growth after which it shows a linear increase, which continues to at least c = 100 mM.

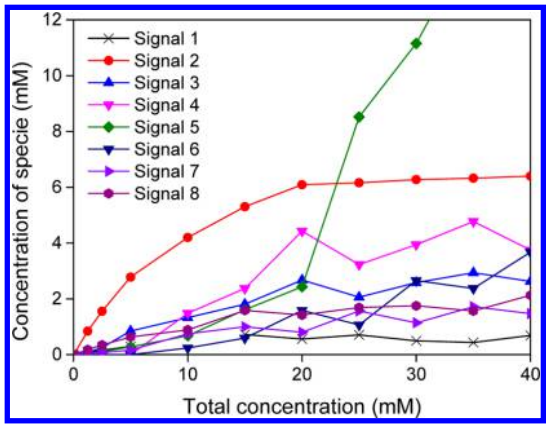

Figure 4. Concentration-dependent behavior of various urethane signals of **1** in $CHCl_3$. The leveling-off of all signals except 5 is indicative for the formation of cyclic species, while the exponential growth of signal 5 is indicative for the growth of a linear polymer.

As shown by Ercolani et al., the leveling off observed for all signals except 5 is indicative for the formation of cyclic structures of a compound with a high dimerization constant,[19] a condition that is indeed met for the UPy end-groups (K_{dim} = 6 × 10^7 M^{-1} in chloroform).[20] In contrast, the linear growth observed for signal 5 is indicative for the formation of linear polymeric species.[18]

In an attempt to discriminate between monomeric, dimeric and possibly higher cyclic structures, the growth rate of the various signals in Figure 4 was examined in more detail (see Figure S3 for details). The results show that the observed cyclic species are mainly monomeric and dimeric in nature and interconvert rapidly. This was further supported by DOSY analysis of a c = 15 mM solution, which showed that the signals associated with monomeric cycles displayed a larger diffusion coefficient than those associated with dimeric cycles (see Figures S10 and S11 for details).

The stability of the monomeric cycles formed by **1** and **2** was studied by determining their effective molarities (EMs), defined as K_{intra}/K_{inter}, and a measure for the stability of a cycle. For urethane-UPy **1** the urethane signals associated with monomeric cycles (i.e., signals 1, 2, and 8) were used. Their combined EM has a value of ±8.5 mM. Since ester-functionalized **2** obviously lacks the urethane protons, a similar deconvolution using the concentration-dependent splitting of UPy proton H_d was performed (see Figure 5). In order to directly compare the results of **2** with **1**, deconvolution was also performed for UPy-urea proton H_d in **1**.

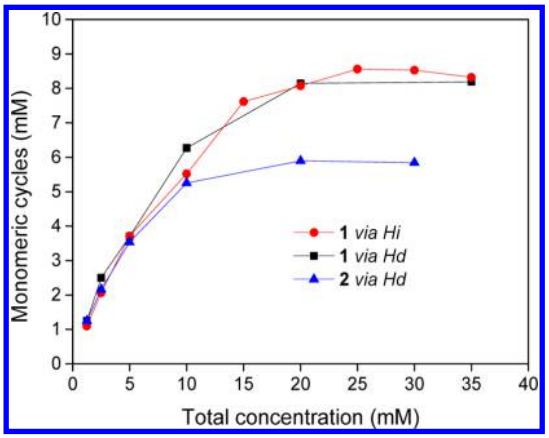

Figure 5. Concentration of monomeric cycles of **1** and **2** versus the total concentration. The position of the plateau that is reached indicates the effective molarity of the compounds.

In compound **1**, the EM values derived from the urethane and the UPy protons are very similar, confirming that proton H_d represents only the monomeric cycles. In contrast, the EM of ester-functionalized **2** reveals a lower value of ±5.8 mM. These results suggest that the monomeric cycles formed by **1** are stabilized by an additional intramolecular interaction. It should be noted that, although only one set of signals for cyclic structures of **2** is observed, it cannot be excluded that multiple species are present.

Molecular modeling reveals an intramolecular UPy–urethane hydrogen bond in the monomeric cycle (Figure 1). In order to experimentally verify the presence of this interaction, DPFGSE-NOESY was performed on a 2.5 mM sample of **1**. This concentration is significantly lower than the EM (8.5 mM), and the solution will therefore contain predominantly monomeric cycles. This experiment revealed a NOE contact between urethane proton H_i and the alkylidene UPy proton H_a, confirming that the intramolecular UPy–urethane hydrogen bond is indeed present. In fact, a very similar UPy–urethane interaction has recently been reported for the crystal structure of the dimeric cycle of a related UPy compound.[21]

As elegantly demonstrated by Butts et al. for strychnine,[22] analysis of NOESY data can be used to accurately estimate proton–proton distances. A similar analysis in our case reveals that the distance between protons H_i–H_a (Figure 1 and Figure S9) is 110% of the distance between protons H_i–H_h, a value that is in close agreement with typical distances (111%) obtained by molecular modeling.

dx.doi.org/10.1021/ma502047h | Macromolecules 2014, 47, 8429–8436

Disrupting the Intramolecular UPy–Urethane Hydrogen Bonds. The material properties of most UPy derivatives reported to date are the result of a hierarchical assembly process consisting of the dimerization of UPy moieties into polymers, lateral stacking of these polymers via hydrogen bonds formed between urethane or urea groups, and last bundling of these stacks into nanofibers (Figure 6).[23]

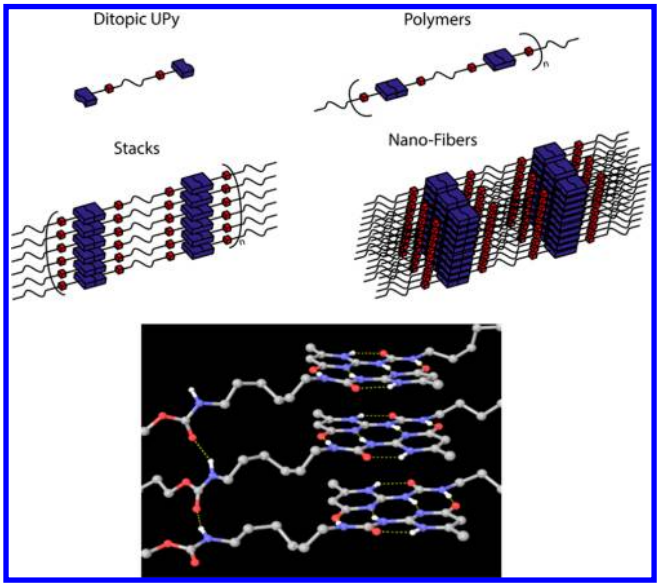

Figure 6. Upper frame: typical assembly process of ditopic UPy compounds. UPy dimerization results in the formation of linear polymers. Stacking of these dimers, stabilized by hydrogen bonding between urethane or urea moieties, results in the formation of stacks. Clustering of these stacks results in nanofibers, giving rise to increased material properties. Lower frame: representation of the UPy stacks with the intermolecular urethane hydrogen bonds present (not the result of a simulation).

In most cases of mechanically induced gelation described in the literature, an intramolecular interaction prevents the molecule from forming supramolecular polymers. The application of mechanical force results in breakage of this interaction, allowing for the growth of nuclei which initiate further aggregation.[17] As described above, such an interaction is indeed present in the majority of the cyclic species formed by **1**. This UPy–urethane interaction might be strong enough to prevent the ring from opening and thus prevent polymerization and eventually gelation of the solution. However, at the concentrations at which the mechanically induced gels are formed (c = 40–120 mM for both the weak and strong gels), the combined cyclic species make up only a small fraction of the solution (≈ 20% for the 100 mM solution), while the rest of the material is present as linear chains. As a result, it is unlikely that the cyclic species are the (only) cause of the mechanically induced gelation.

The above analysis prompted us to hypothesize that a similar UPy–urethane interaction as observed in the cyclic species would also be present in the linear polymers (Figure 7). This would occupy the urethane NH and as thus prohibit the formation of lateral urethane–urethane interactions, shown to be vital for the formation of stable UPy stacks[23,24] and in good agreement with the fact that ester-functionalized **2** is unable to form gels. In that case, the UPy–urethane hydrogen bonds would be present in the linear species in solution but absent in

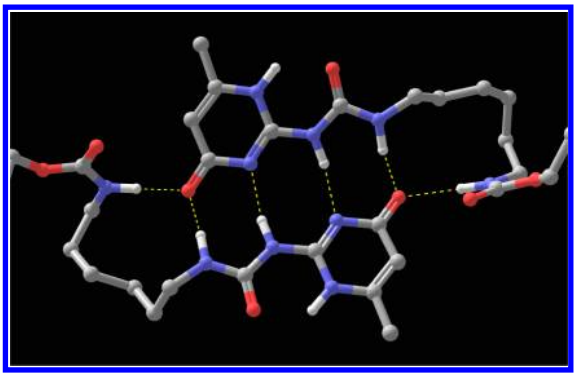

Figure 7. Representation of the proposed UPy–urethane interaction in the linear species (not the result of a simulation).

the gel. To verify this, DPFGSE-ROESY measurements were performed on the linear species in a 60 mM solution of **1** and on all species in the corresponding strong gel, which was made by stirring the solution for 3 h. For proper comparison both measurements were performed on a magic-angle-spinning setup. The result of the measurements on the linear species in solution revealed a very similar NOE contact as was observed for the cyclic species in the 2.5 mM sample. In contrast, the measurements performed on the strong gel did not show a NOE contact between proton H_i and H_a.

Additional investigation of c = 2.5 mM and c = 60 mM slowly cooled solutions of **1** by IR spectroscopy revealed two N–H stretch bands at ν = 3450 and 3220 cm^{-1}, of which the 3450 cm^{-1} vibration can be attributed to a non-hydrogen-bonded urethane (Figure 8).[25,26] The value of 3220 cm^{-1} is low

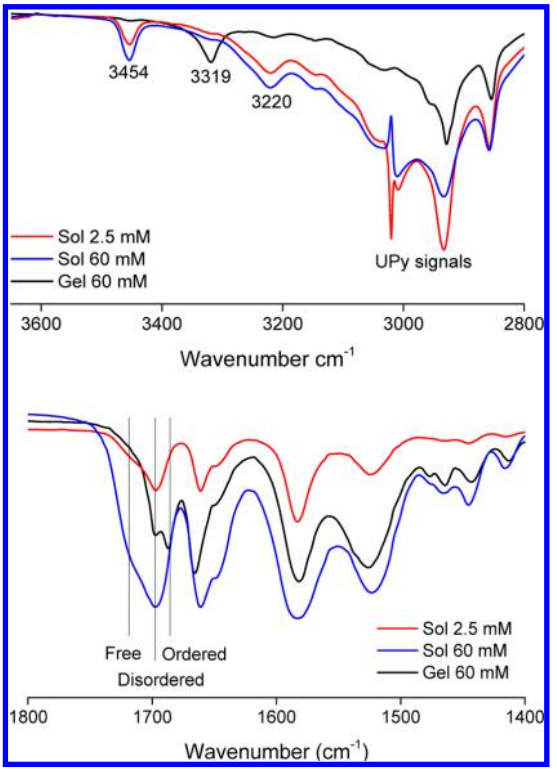

Figure 8. Zoom of FT-IR spectra of **1** in $CHCl_3$ (rescaled for clarity). Liquid samples were measured in solution l = 0.05 cm. The strong gel was measured in ATR mode. The spike at 3050 cm^{-1} is an artifact resulting from the absorption of the sample holder.

dx.doi.org/10.1021/ma502047h | Macromolecules 2014, 47, 8429–8436

compared to the value of 3300 cm^{-1} typically found in polyurethanes.[25,26] This may be caused by the fact that the urethane group in our system acts only as a hydrogen bond donor (the C═O part of the urethane is not participating in any hydrogen bonds). In contrast, IR studies on the strong gel formed by extended stirring showed the absence of both peaks and the appearance of a new N−H peak at ν = 3319 cm^{-1}, which can be attributed to the formation of lateral urethane−urethane hydrogen bonds.[25,26]

According to Painter et al., three different signals corresponding to urethane C═O stretch vibrations can be observed:[26] a signal corresponding to a non-hydrogen-bonded C═O at ν = 1721 cm^{-1}, a disorderly bound C═O at ν = 1699 cm^{-1}, and an orderly bound C═O at ν = 1684 cm^{-1}. As shown in Figure 8, signals corresponding to a free and disorderedly hydrogen-bonded urethane are observed for the c = 2.5 and c = 60 mM solutions, in agreement with the observations in the N−H regime. Also similar as in the N−H regime, the free C═O is absent in the strong gel while a band for the ordered state has emerged. It should be noted that a signal corresponding to the disorderly bound C═O is also still present. While this could originate from disordered sections of the gel, it is also the position of the C═O vibration in the "urea" part of the UPy moiety.[25,27]

Similar measurements were also performed for the weak gel, formed by sonication or stirring for 10 min. These revealed identical NMR and IR spectra as observed for the solution. This suggests that only a very small fraction of the linear UPy polymers is stacked, in good agreement with the low strength of this gel. In order to investigate if the strong gel formed by **1** indeed comprises bundles of stacked polymers, WAXS was performed on the dried gel (c = 80 mM). As a reference, compounds with urethane−urethane linker lengths of C_8 and C_{16} instead of C_{12} were synthesized according to a literature procedure and measured as well.[17] The results revealed signals which have previously been attributed to interchain distances in polyurethanes, interdimer UPy−UPy distances, and stack−stack distances in UPy nanofibers. Hence, evidence is presented to support the proposed structure of the gel as presented in Figure 6 (see Figure S13 for more details).

In order to study the gels directly (i.e., without drying), polarized optical microscopy (POM) was used to characterize a weak gel made by sonication and strong gel made by stirring (c = 60 mM, Figure 9). POM analysis revealed that the weak gel does contain some birefringent sections but is generally very unordered and heterogeneous. In contrast, the strong gel is not birefringent at all but appears much more homogeneous. This suggests that the continued sheer stress applied by extended stirring allows the heterogonous sections of the weak gel to re-form in a more ordered and dense network, very similar as has been reported in the literature.[16]

Mechanical Properties of the Strong Gel. With the molecular structure of the gels understood, we focused on studying their material properties using oscillatory rheology. The fragile structure of the weak gel made it impossible to obtain reproducible results. Therefore, further experiments were performed on a strong gel, formed by stirring an 80 mM solution of **1** in chloroform for 3 h. Frequency sweep measurements (ω = 0.5−100 rad/s, γ = 1%) revealed that the storage modulus is larger than the loss modulus over the complete range of the experiment, showing the elastic properties of the gel. Strain sweep experiments show that the crossover point lies at a strain of 12% (ω = 1 rad/s). In addition, the thixotropic nature of the gel was examined by alternating between low (1%) and high (100%) strain. The gel heals partly in ±40 s, and this process is reproducible (Figure 10). The slow drift in G' and G'' is attributed to incomplete healing of the gel and/or evaporation of the solvent, leading to shrinkage of the gel and a reduced contact area with the setup.

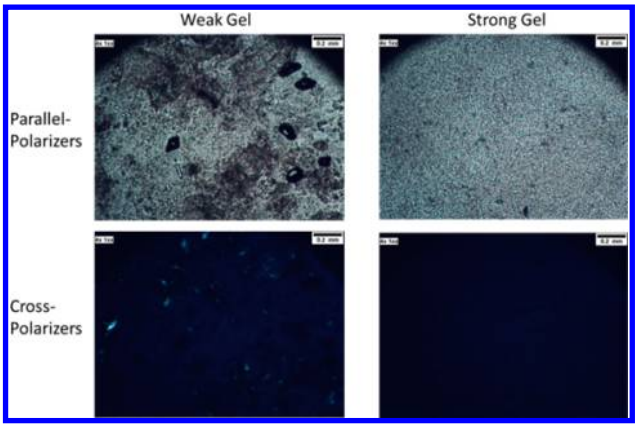

Figure 9. Polarized optical microscopy pictures of a weak gel made by sonication for 10 min and a strong gel made by stirring for 3 h (c = 60 mM). Both gels were allowed to equilibrate for 24 h before analysis. Magnification is 4×; scale bar represents 0.2 mm.

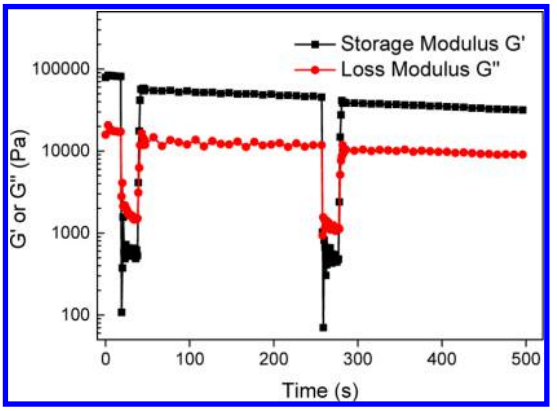

Figure 10. Thixotropic properties of the c = 80 mM gel of **1** in $CDCl_3$ formed by stirring for 3 h and a resting period of 2 h. The measurement was performed using a 25 mm parallel plate setup, consisting of strains of 10 s 1%; 20 s 100%; 200 s 1%; 20 s 200%; and 100 s 1%. ω = 1 rad/s. See Supporting Information for further experimental details.

Proposed Mechanism for the Gelation of 1. The results presented herein indicate that a UPy−urethane interaction is present in both cyclic and linear species in solution but is absent in the strong gel. This interaction most likely kinetically traps urethane-UPy **1**, thereby preventing the formation of lateral aggregates, necessary for gelation.[23,24] This might partly be the result of sterical hindrance as a result of back-folding of the polymeric chain but likely more significantly arise from occupation of the urethane moieties in the UPy−urethane hydrogen bonds.

One mechanism for the gelation that we considered is the mechanically induced breakage of laterally stacked UPy aggregates. This would lead to a large increase in the number of aggregates, which could act as nuclei for further aggregation. However, as mentioned above, it is unlikely that many lateral aggregates are formed while the UPy−urethane hydrogen

dx.doi.org/10.1021/ma502047h | Macromolecules 2014, 47, 8429−8436

bonds are present in the cyclic structures or supramolecular polymers. Furthermore, if the above mechanism is correct, it would effectively lead to a multiplication of similar structures and would therefore not explain the absence of the UPy–urethane interaction in the gel as shown by NOE and IR. For the initiation of the gelation process, therefore, another mechanism is required.

For this reason it is more likely that the linear structures in solution are initially nonstacked one-dimensional polymers. Stretching or breaking the linear polymer by the applied mechanical stress likely results in breakage of the UPy–urethane interactions. In turn, the loss of this interaction allows for the formation of a nucleus containing stacked UPy dimers, stabilized by urethane–urethane hydrogen bonds. This nucleus then induces the growth of larger structures, eventually leading to the mechanically induced gelation of the solution. The fact that only continued stirring leads to the formation of the strong gel can be explained by a higher degree of physical cross-links. This not only leads to a stronger gel but also to larger aggregates, explaining the opaque appearance of this gel. In other words, due to the high viscosity, the weak gel is also kinetically trapped structure on its way to a strong gel.

The formation of weak gels as a result of quenching has been reported before,[16] where the low mechanical strength of the gel was attributed to the formation of many nucleation sites as a result of the fast cooling, thereby leading to large amorphous sections. This is a very plausible explanation for the weak material properties of our gel as wel. In contrast to the reported system, our system does not gelate as a result of slow cooling, suggesting that nucleation only takes place at or around the melting point of chloroform. The gelation as a result of fast cooling by immersion in liquid nitrogen might be explained as the result of a shift in activation barriers for the formation of the structures found in the slowly cooled liquid and gel state as a function of temperature. However, the slowly cooled liquid samples also form a similar weak gel as a result of cooling in liquid nitrogen. Furthermore, fast cooling the hot or ambient solutions by immersing in ice–water or cold chloroform (T = −45 °C) did not result in gelation, similar as removal of the vial from the liquid nitrogen before crystallization of the solvent had occurred. For this reason it is more likely that, rather than a change in activation barriers, the crystal growth of chloroform is responsible for the observed gelation. If the chloroform crystals indeed act as nuclei for the gelation, their large number might also explain why the gelation as a result of cooling proceeds in several minutes, instead of the hours that are necessary for the gelation as a result of mechanical agitation to take place. Another plausible explanation is related to the large increase in the relative permittivity (i.e., dielectric constant) of chloroform as a result of the decrease in temperature.[28,29] It is possible that at a temperature close to its freezing point the polarity of the solvent increases to a point where the solubility of **1** is strongly decreased, thereby inducing gel formation.

■ CONCLUSIONS

Ditopic UPy **1** forms a variety of different cyclic species in slowly cooled solutions, primarily comprising different conformations of monomeric and dimeric cycles. NOESY and FT-IR data show that the majority of these cycles are stabilized by an intramolecular UPy–urethane hydrogen bond. A very similar interaction is also observed in the linear polymers formed at higher concentration. As observed by WAXS, NOESY, and FT-IR, the application of mechanical force results in the formation of a gel made of fibers of stacked UPy dimers, with the UPy–urethane interaction no longer present. These results show that the UPy–urethane hydrogen bonds kinetically trap the compound, while mechanical force disrupts these interactions, allowing for the formation of a stacked nucleus on which larger structures can grow, leading to gelation of the solution. Fast cooling of the solutions results in gelation even when no mechanical stress is applied. Experimental observations show that this phenomenon only happens when the solvent is (nearly) frozen. Likely explanations are therefore either a nucleation process initiated by the solvent crystals or gelation as a result of the increase in the dielectric constant of the solvent as a result of the decrease in temperature. The work presented here provides further insight into the influence of mechanical stresses on supramolecular systems and will contribute to the development of stimuli-responsive materials.

■ ASSOCIATED CONTENT

Supporting Information

WAXS, rheology, and FT-IR analysis. This material is available free of charge via the Internet at http://pubs.acs.org.

■ AUTHOR INFORMATION

Corresponding Author

*E-mail e.w.meijer@tue.nl (E.W.).

Notes

The authors declare no competing financial interest.

■ ACKNOWLEDGMENTS

This work is financed by The Netherlands Organisation for Scientific Research (NWO-TOP grant: 10007851), the Dutch Ministry of Education, Culture and Science (Gravity program 024.001.035), and the European Research Council (FP7/2007–2013, ERC Advanced Grant No. 246829).We thank Dr. Wesley R. Browne for useful discussions about the gelation induced by fast cooling.

■ REFERENCES

(1) Stuart, M. A. C.; Huck, W. T. S.; Genzer, J.; Muller, M.; Ober, C.; Stam, M.; Sukhorukov, G. B.; Szleifer, I.; Tsukruk, V. V.; Urban, M.; Winnik, F.; Zaucher, S.; Luzinov, I.; Minko, S. *Nat. Mater.* **2010**, *9*, 101–113.

(2) Kumar, G. S.; Neckers, D. C. *Chem. Rev.* **1989**, *89*, 1915–1925.

(3) Schmaljohann, D. *Adv. Drug Delivery Rev.* **2006**, *58*, 1655–1670.

(4) Misra, A.; Stein, R. S. J. *J. Polym. Sci., Polym. Phys. Ed.* **1979**, *17*, 235–257.

(5) Kondepudi, D. K.; Kaufman, R. J.; Singh, N. *Science* **1990**, *250*, 975–976.

(6) Noorduin, W. L.; Izumi, T.; Millemaggi, A.; Leeman, M.; Meekes, H.; van Enckevort, W. J. P.; Kellog, R. M.; Kaptein, B.; Vlieg, E.; Blackmond, D. G. *J. Am. Chem. Soc.* **2008**, *130*, 1158–1159.

(7) Giri, G.; Verploegen, E.; Mannsfeld, S. C. B.; Atahan-Evrenk, S.; Kim, D. H.; Lee, S. Y.; Becerril, H. A.; Aspuru-Guzik, A.; Toney, M. F.; Bao, Z. *Nature* **2011**, *480*, 504–508.

(8) Mahmoudi, T.; Karimkhani, V.; Seok Song, G.; Soo Lee, D.; J. Stadler, F. *Macromolecules* **2013**, *46*, 4141–4150.

(9) Carnall, J. M. A.; Waudby, C. A.; Belenguer, A. M.; Stuart, M. C. A.; Peyralans, J. J.-P.; Otto, S. *Science* **2010**, *327*, 1502–1506.

(10) Xu, J.-F.; Chen, Y.-Z.; Wu, D.; Wu, L.-Z.; Tung, C. H.; Yang, Q.-Z. *Angew. Chem.* **2013**, *52*, 9920–9924.

(11) Paulusse, J. M. J.; Sijbesma, R. P. *J. Polym. Sci., Part A: Polym. Chem.* **2006**, *44*, 5445–5453.

(12) Cabane, B.; Wong, K.; Lindner, P.; Lafuma, F. J. *Rheology* **1997**, *41*, 531–547.

(13) Xie, D.; Wu, H.; Zaccone, A.; Braun, L.; Chen, H.; Morbidelli, M. *Soft Matter* **2010**, *6*, 2692−2698.
(14) Piepenbrock, M.-O. M.; Clarke, N.; Steeds, J. W. *Soft Matter* **2010**, *6*, 3541−3547.
(15) Herpt, J. T.; Stuart, M. C. A.; Browne, W. R.; Feringa, B. L. *Langmuir* **2013**, *29*, 8763−8767.
(16) Weng, W.; Beck, J. B.; Jamieson, A. M.; Rowan, S. J. *J. Am. Chem. Soc.* **2006**, *128*, 11663−11672.
(17) Cravotto, G.; Cintas, P. *Chem. Soc. Rev.* **2009**, *38*, 2684.
(18) Llansola, F. R.; Meijer, E. W. *J. Am. Chem. Soc.* **2013**, *135*, 6549−6553.
(19) Ercolani, G.; Mandolini, L.; Mencarelli, P.; Roelens, S. *J. Am. Chem. Soc.* **1993**, *115*, 3901−3908.
(20) Söntjes, S. H. M.; Sijbesma, R. P.; Genderen, M. H. P.; Meijer, E. W. *J. Am. Chem. Soc.* **2000**, *122*, 7487−7493.
(21) Lafitte, V. G. H.; Aliev, A. E.; Horton, P. N.; Hursthouse, M. B.; Hailes, H. C. *Chem. Commun.* **2006**, 2173−2175.
(22) Butts, C. P.; Jones, C. R.; Towers, E. C.; Flynn, J. L.; Appleby, L.; Barron, N. *Org. Biomol. Chem.* **2011**, *9*, 177−184.
(23) Appel, W. P. J.; Portale, G.; Wisse, E.; Dankers, P. Y. W.; Meijer, E. W. *Macromolecules* **2011**, *44*, 6776−6784.
(24) Kautz, H.; van Beek, D. J. M.; Sijbesma, R. P.; Meijer, E. W. *Macromolecules* **2006**, *39*, 4265−4267.
(25) Coleman, M. M.; Lee, K. H.; Skrovanek, D. J.; Painter, P. C. *Macromolecules* **1986**, *19*, 2149−2157.
(26) Lee, H. S.; Wang, Y. K.; Hsu, S. L. *Macromolecules* **1987**, *20*, 2089−2095.
(27) Dankers, P. Y. W.; Adams, P. J. H. M.; Löwik, D. W. P. M.; van Hest, J. C. M.; Meijer, E. W. *Eur. J. Org. Chem.* **2007**, 3622−3632.
(28) Philippe, R.; Piette, A. M. *Bull. Soc. Chim. Belg.* **1955**, *64*, 600−627.
(29) West, R. C. In *Handbook of Chemistry and Physics*, 60th ed., 2nd printing; Chemical Rubber Co.: Boca Raton, FL, 1980.